

A precise and user-independent quantification technique for regional comparison of single volume proton MR spectroscopy of the human brain

Gunther Helms*

MR Research Center, Department of Clinical Neuroscience, Karolinska Institute, Stockholm, Sweden

Received 10 February 2000; revised 26 June 2000; accepted 30 August 2000

ABSTRACT: The aim of this work was to study and correct the influence of varying coil load and local B_1 field in single volume MR spectroscopy. A simple, precise, and user-independent way to adjust the transmitter gain has been developed and validated. It is based on a fit of the localized signal to flip angle variation around 90° . This method proved to be robust against B_1 gradients and suitable for *in vivo* applications. Local B_1 correction was combined with an external reference and decomposition of the volume into CSF and tissue to obtain a comprehensive absolute quantification of tissue water content and metabolite concentrations in human brain. STEAM localized spectra of parietal and insular gray matter and subparietal white matter ($n = 11$, $TE = 30$ ms) were analyzed using a linear combination of model spectra (LCModel). Coefficients of variation (CV) between 1.5% and 4% were obtained for the tissue water content (1–2% in a single subject). The CVs of major metabolite concentrations (4–21%) were dominated by the errors of the spectral analysis.

The largest B_1 variation in the *in vivo* experiments (range 30%) was due to changes in coil load. Differences in regional sensitivity due to B_1 inhomogeneity (parietal: 8% and 9%; insular: 16%) were found to be the second largest source of variation. Correction for local B_1 improved standard deviations and intra-subject reproducibility. On average, sensitivity was 9% less in insular than in parietal gray matter. If ignored, significant differences were introduced for water and N-acetyl-aspartate or were obscured for creatine and choline. Hence, local sensitivity correction proved to be necessary for regional comparison of absolute metabolite concentrations.

Copyright © 2000 John Wiley & Sons, Ltd.

KEYWORDS: proton spectroscopy; human brain; absolute quantification; regional comparison; RF inhomogeneity

INTRODUCTION

Although the theory of the NMR signal is well understood^{1,2} there is no general agreement on a quantification procedure for *in vivo* proton MR spectroscopy (MRS). Changes of the sensitivity, i.e. the relation between NMR signal strength and transverse magnetization M_{tr} , are caused by the interaction of the RF hardware and the

sample. They have to be corrected in order to yield comparability between different experiments. Absolute quantification generally consists of two steps: correction of the measured signal S for changes of the sensitivity; and calibration of the corrected signal S_{corr} with a standard of known concentration.⁶ Sensitivity correction yields a quantification in arbitrary 'institutional' units, which are then converted into absolute molar units obtained from the standard.

The quantification techniques published so far differ mainly in the way the sensitivity is corrected: using an external^{3–5} phantom, which by necessity is placed on the fringes of the RF coil, involves the assumption of negligible RF inhomogeneity.⁸ If the principle of reciprocity between the normalized B_1 field and the sensitivity is used,^{6,7} it is assumed that there are no long-term changes and that the coil has constant impedance, i.e. is reliably matched and tuned.⁸ Although the reciprocity principle can be used to correct for RF inhomogeneity,⁷ this may not be fully accounted for if the amplitude of a non-selective reference pulse is used.^{6,8}

The aim of this work was to strengthen the reliability

*Correspondence to: G. Helms, MR Centrum N8, Karolinska Hospital, SE-17176 Stockholm, Sweden.

E-mail: gunther@mrc.ks.se

Contract/grant sponsor: Deutsche Forschungsgemeinschaft; contract grant number: He 2638/1-1)

A preliminary account of this work has been presented: Helms G. Local sensitivity correction in quantitative localized MRS of the human brain. *Proc. Int. Soc. Magn. Reson. Med.* 1997; 5: 1404.

Abbreviations used: Cho, choline containing compounds; CSF, cerebro-spinal fluid; CV, coefficient of variation; ins GM, insular gray matter; pa WM, parietal white matter; pmp GM, paramedian-parietal gray matter; RF, radio-frequency; R_{tra} , linear transmitter reference; SD, standard deviation; SNR, signal-to-noise ratio; SPGR, spoiled gradient echo; STEAM, stimulated echo acquisition mode; tCr, total creatine; TG, transmitter gain; tNAA, total N-acetyl aspartate; TWC, tissue water content; VOI, volume of interest.

of quantification by avoiding assumptions on the MR system's RF hardware and on the performance of the pre-scan routines which calibrate the flip angle. For this purpose, we developed a precise and user-independent method to determine the local sensitivity from the *localized* water signal. The theoretical flip angle dependence of the localized signal was fitted to a few unsuppressed scans obtained at various values of the RF amplifier's transmitter gain (TG). The correct TG at the location of the VOI is determined from the maximum of the localized signal, and thus independent of system or user adjustments. From this value, a measure is derived for the sensitivity of the MR signal for each VOI according to the local nature of the reciprocity principle. This made it possible to study the effects of RF inhomogeneity on the quantification of single volume MRS data.

A quantification technique is suggested to eliminate the influence of RF inhomogeneity, long-term changes and coil impedance on the MR signal. Sensitivity changes are corrected by a *combination* of external reference and the principle of reciprocity. The method was validated in phantom experiments and was used to quantify tissue water and metabolites from STEAM⁹ localized proton spectra of parietal and insular gray matter and parietal white matter.

THEORY

The proportionality between the RF current I_{tra} that is fed into the coil and the resulting magnetic field $B_1(x)$ is fundamental for both excitation and reception sensitivity. It is conveniently described by the normalized RF field $B_1(x)/I_{\text{tra}}$, but neither B_1 nor I_{tra} can be determined in normal console operation. $B_1(x)/I_{\text{tra}}$ changes with coil load, and the transmitted voltage U_{tra} has to be scaled accordingly to match flip angles α with their nominal values α_{nom} . In this work we derive a measure for $B_1(x)/I_{\text{tra}}$ from the adjustment of the transmitter amplification, which for the sake of generality is expressed as a *linear* transmitter reference R_{tra} . Dependent on the MR system, either the peak voltages of the RF pulses or a transmitter gain is accessible to the operator. Peak voltages depend on the RF pulse and flip angle, but may be used directly if they refer to a 'reference pulse' of consistent duration, shape and flip angle. Transmitter gains are often independent of pulse shape and flip angle, but given in logarithmic decibel units, which have to be linearized to yield proportionality to $B_1(x)/I_{\text{tra}}$.

Inhomogeneity of the RF field is, of course, not adequately described by a single R_{tra} value. Spatial variation of $B_1(x)/I_{\text{tra}}$ will result in a corresponding distribution of flip angles. Let $R_{\text{tra}}(x)$ be the transmitter reference that gives correct flip angles at point x . Deviations from the nominal flip angle correspond to the mismatch of the chosen transmitter reference

$R_{\text{tra}}^{\text{nom}}$ from $R_{\text{tra}}(x)$:

$$\alpha(x) = \alpha_{\text{nom}} \frac{R_{\text{tra}}^{\text{nom}}}{R_{\text{tra}}(x)}. \quad (1)$$

In this study we vary $\alpha(x)$ by $R_{\text{tra}}^{\text{nom}}$ in order to determine the local $R_{\text{tra}}(x)$ from the flip angle dependence of the localized signal. Because R_{tra} refers to the transmitted voltage $U_{\text{tra}} = Z I_{\text{tra}}$ (and not to the current), the coil impedance Z may have to be taken into account:

$$R_{\text{tra}}(x) \propto \frac{I_{\text{tra}} \cdot Z}{B_1(x)}. \quad (2)$$

According to the reciprocity between transmission and reception,^{1,2} the normalized RF field $B_1(x)/I_{\text{tra}}$ at point x also governs the local sensitivity, i.e. the signal S induced by transverse magnetization $M_{\text{tr}}(x)$. In single volume MRS, the VOI is small compared to coil dimensions, and RF homogeneity can be assumed across the volume V :

$$\frac{S}{V} \propto \frac{B_1}{I_{\text{tra}}} \cdot M_{\text{tr}}. \quad (3)$$

In the following V , M_{tr} , B_1/I_{tra} are considered for a given VOI. The spatial dependence is omitted to simplify the equations. Of note, these parameters may differ between different VOIs. The problem of sensitivity correction is to find a suitable experimental estimation of B_1/I_{tra} that establishes proportionality between the corrected signal and M_{tr} . Use of eq. (2) yields

$$S \cdot \frac{R_{\text{tra}}}{V} \propto Z \cdot M_{\text{tr}}, \quad (4)$$

which is used to correct the signal for the VOI specific parameters V and R_{tra} , i.e. the local B_1 field. This correction allows the signal from different VOIs to be compared within one examination. However, Z may change with the coil load of each individual experiment or due to errors of the tuning and matching procedure. These inter-experimental changes can be monitored by a reference measurement in a stable external phantom.³⁻⁵ After correction with $R_{\text{tra}}^{\text{ext}}$ and V^{ext} , the external reference signal S^{ext} may be used as a measure for Z :

$$S^{\text{ext}} \cdot \frac{R_{\text{tra}}^{\text{ext}}}{V^{\text{ext}}} \propto Z. \quad (5)$$

Moreover, the proportionality in eqs. (2)–(5) may be subject to long-term RF changes, e.g. aging of the amplifier tube or change of hardware components. These will require a repetition of the calibration, if the correction is based on the principle of reciprocity only. The final correction

$$S_{\text{corr}} = \frac{S \cdot R_{\text{tra}} \cdot V^{\text{ext}}}{S^{\text{ext}} \cdot R_{\text{tra}}^{\text{ext}} \cdot V} \propto M_{\text{tr}} \propto \text{concentration} \quad (6)$$

eliminates RF inhomogeneities as well as impedance and long-term changes to render S_{corr} proportional to the

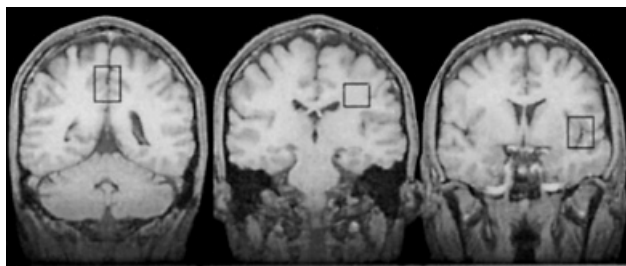


Figure 1. Typical VOI positions on coronal three-dimensional SPGR images: paramedian-parietal gray matter (pmp GM), parietal white matter (pa WM) and insular gray matter (ins GM) (left to right)

concentration. Arbitrary factors and systematic errors of R_{tra} will cancel by division, as well as deviations of V from the nominal value, if the same localization is applied.

MATERIALS AND METHOD

The study was performed on a 1.5 T clinical MR system (Signa Advantage, General Electric Medical Systems, Milwaukee, WI) using the standard quadrature transmit/receive birdcage head coil. No individual tuning and matching was performed. T_1 -weighted three-dimensional spoiled gradient echo (SPGR) images ($TR/TE/\alpha = 18 \text{ ms}/4.8 \text{ ms}/20^\circ$) in coronal view were used to position the VOIs for STEAM localization ('steamcsi', release 5.4.3). Eleven VOIs of gray matter (GM) in the paramedian-parietal (pmp) and the insular (ins) region, as well as parietal white matter (pa WM) were examined. Typical VOI positions are shown in Fig. 1. The VOIs were individually adjusted to minimize gray/white matter partial volume effects. VOI size was between 6 ml and 17 ml with average volumes of 13.1 ml (pa GM) 10.7 ml (ins GM) and 9.1 ml (pa WM). Time parameters were $TR/TE/TM = 6000/30/13.7 \text{ ms}$ for conventional averaging of 64 water suppressed scans. Optimized RF pulses were used for slice selection and water suppression.¹⁰ The bandwidth of the water suppression pulses had been reduced to 40 Hz in order to preserve the methylene singlet of creatine. All acquisitions were recorded at maximum receiver gain, which made corrections for different receiver settings unnecessary. Seventeen young healthy adults (12 male/5 female) aged between 22 and 32 years (mean 26 years) were examined in two regions according to the ethical guidelines of the Karolinska Hospital. Another male volunteer (27 years) was examined five times in all three regions to study intra-subject reproducibility.

The spectroscopy protocol comprised manual shimming on the localized water signal, manual adjustment of the water suppression, acquisition of a reference scan for eddy current correction and two series of single acquisitions of unsuppressed water signal. In the first

series ('TG series') the transmitter gain was varied through 40, 55, 70, 85, 100 and 115 (system units, tenth of decibel). The second series ('TE series') consisted of eight acquisitions at echo times of 30, 45, 67, 100, 200, 500, 900 and 1500 ms to allow estimation of the size of water compartments in the VOI as described in Ernst *et al.*⁴. The time between two acquisitions was 15 s. Thus, the additional time required for quantification was 1.5 min for each TG series and 2 min for each TE series. The water signal was measured as the maximum of the acquired half echo, which is displayed after acquisition as the fraction of the dynamic range of the analog-digital converter. In these series, the STEAM sequence was run without suppression to avoid arbitrary saturation due to RF leakage from the unblanked transmitter. If the amplitude of the long suppression pulses was set to zero, the water was found to be up to 20% saturated.

A water-filled glass sphere of 6 cm diameter was mounted at a reproducible position on the coil axis behind the subject's head. In order to achieve reproducible B_0 conditions, the patient's bed was moved to position the sphere at magnet isocenter and a pre-defined set of shim currents was loaded. A TG series was then acquired from a cubic VOI of 1.7 cm side in the external phantom.

Postprocessing

System TG values in tenths of decibel were linearized using

$$R_{\text{tra}} = 10^{(\text{TG}/200)} \quad (7)$$

In this study the flip angle is varied by changing TG for $\alpha_{\text{nom}} = 90^\circ$ and observed indirectly through the flip angle dependence of the STEAM signal:

$$S \propto \sin^3 \alpha = \sin^3 \left(90^\circ \frac{R_{\text{tra}}^{\text{nom}}}{R_{\text{tra}}} \right) \quad (8)$$

where the chosen values are denoted by $R_{\text{tra}}^{\text{nom}}$. Equation (8) was fitted to the TG series both in the external phantom and the VOIs. From the fitted curves the water signal at 90° flip angle and the transmitter reference R_{tra} were determined, i.e. the signal maximum and its position. The water signal of the TE series was then scaled according to eq. (6) by the volume size, R_{tra} and the reference signal. The deviation from the ideal 90° flip angle as expressed in eq. (8) was also corrected for. A biexponential decay was then fitted to the data points of the TE series. The Levenberg-Marquardt algorithm was used for nonlinear least-square fitting. The component with short T_2 of the biexponential fit of the TE series was assigned to tissue water, the long T_2 component to CSF.^{3,4} Some of the WM VOIs contained little CSF, which prevented a reproducible fit of the long T_2 component. Using the estimate of CSF T_2 from the GM voxels (950 ms) revealed CSF contributions of less than

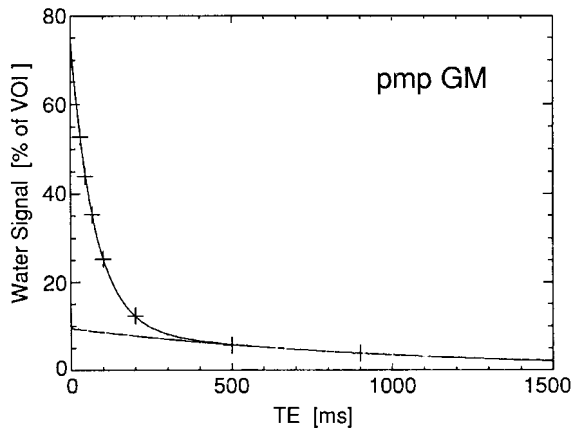


Figure 2. Biexponential fit to the unsuppressed water signal measured at various TE in pmp GM. The signal is given relative to 100% water in the VOI. Up to 16% CSF was observed in the gray matter VOIs

2% in accordance with Ernst *et al.*⁴. The T_2 corrected amplitudes were expressed as fractional water signal s_{tissue} and s_{CSF} compared to 100% water in the VOI (Fig. 2). Assuming full MR ‘visibility’ of the CSF signal, s_{CSF} equals the fraction of the VOI containing CSF. V was replaced by the partial tissue volume

$$V_{\text{tissue}} = (1 - s_{\text{CSF}}/100\%) \cdot V \quad (9)$$

in order to estimate average tissue concentrations of metabolites. Relating s_{tissue} to V_{tissue} yielded the tissue water content

$$\text{TWC} = s_{\text{tissue}} / (1 - s_{\text{CSF}}/100\%) \quad (10)$$

The water suppressed time domain data was corrected for phase distortions¹¹ and analyzed in the ppm region between 1.0 and 4.0 ppm using the LCMoel program¹² without further correction for relaxation effects. Details of the spectral analysis have been published elsewhere.¹³ Typical spectra from the three regions are shown in Fig. 3. For calibration the same protocol as *in vivo* was run on a phantom containing a solution of brain metabolites.¹³ A spectrum with high signal-to-noise and a TE series was scaled accordingly and used as a standard for molar metabolite concentrations and 100% water.

RESULTS

Phantom experiments

Linearity of the localized signal to slice thickness was excellently obeyed in the range between 6 and 40 mm (deviations < 1%, Pearson’s coefficient of correlation $r > 0.999$). B_0 inhomogeneities may distort the shape of the selected VOI or change the refocusing and thus influence the localized signal. Shimming the linear coils

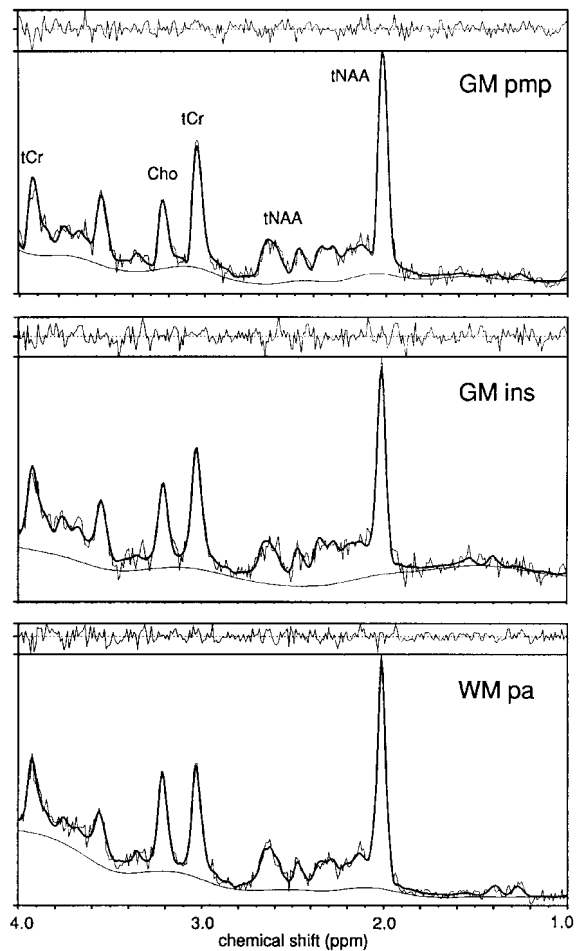


Figure 3. LCMoel analysis of typical spectra obtained at $TE = 30$ ms from paramedian-parietal gray matter (pmp GM), parietal white matter (pa WM), and insular gray matter (ins GM) of one subject. Not to scale. The top traces show the residues of the fit. The main metabolites have been assigned in the spectrum of pmp GM

changed the localized signal less than 1%. Figure 4A shows the signal over a wide range of TG values together with the fitted $\sin^3 \alpha$ curve. The somewhat larger signal measured for very small and very large TG are caused by changes in the slice profile due to the nonlinearity of the excitation.

To verify the applicability of the fitting method in off-center positions (i.e. in the external phantom), the phantom was centered at the lower opening of the head coil and different positions on the coil axis were examined in the gradient of the RF field. When necessary the number of TG points was extended until flip angles greater than 90° were reached to warrant an accurate determination of the maximum. The signal from a VOI position 8 cm outside the head coil illustrates the effect of an B_1 gradient across the VOI (Fig. 4B). For small flip angles the $\sin^3 \alpha$ dependence is well obeyed by the average signal, because the B_1 gradient creates a signal gradient across the VOI. With the flip angle approaching

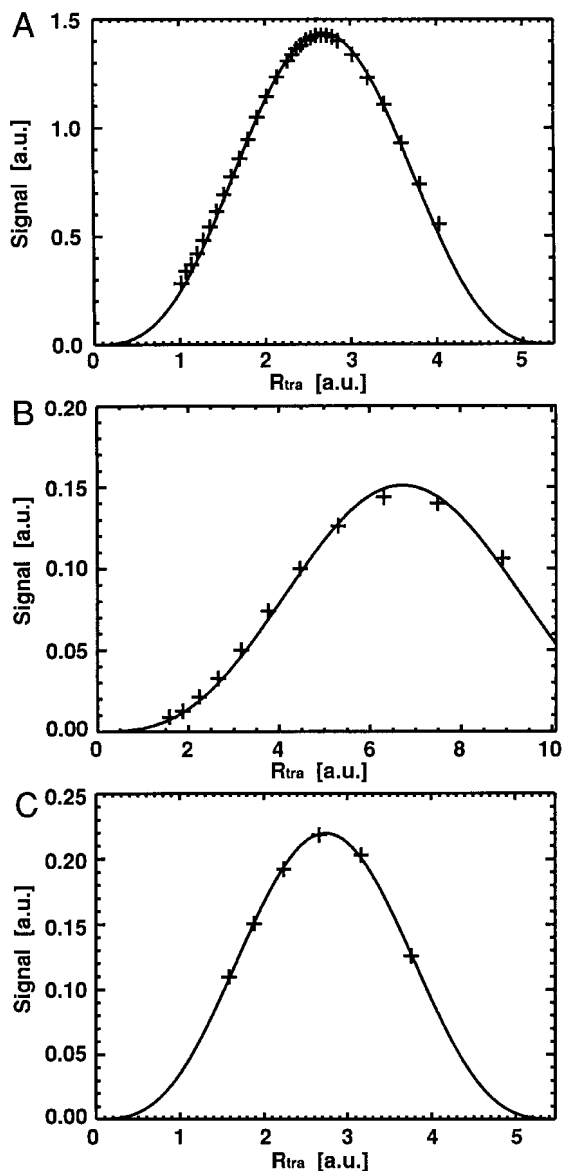


Figure 4. (A) The localized STEAM signal at coil center measured in a phantom over a wide range of TG values. The x-axis shows R_{tra}^{nom} in linear scale [eq. (7)]. The RF pulses were optimized for 90° excitation. The fitted $\sin^3\alpha$ dependence is excellently followed between 70° and 110° and well followed between 45° and 145° . Deviations at higher and lower flip angles are caused by the nonlinearity of the slice excitation. Reducing the range of points changed the fitted parameters by less than 1%. (B) The localized STEAM signal in the presence of a strong B_1 field gradient. Around the maximum the signal is markedly reduced due to incomplete excitation on both sides of the VOI. At lower flip angles the flip angle gradient is averaged out across the VOI. (C) The $\sin^3\alpha$ curve fitted to six points measured *in vivo* as defined by the TG series of the protocol. R_{tra} can be determined within 1.5%

90° the signal distribution is flattened on one side and finally becomes convex. Consequently, the average signal from the VOI is decreased at the maximum and appears below the fitted curve. R_{tra} was 2.8 higher than at

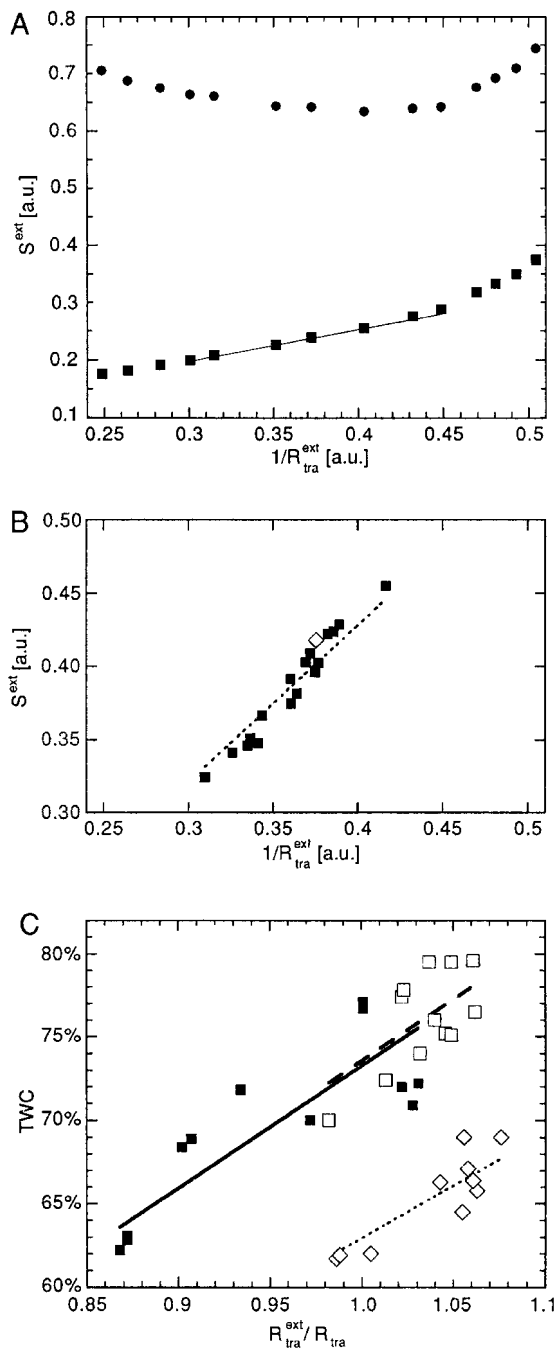


Figure 5. Scatter plots of the localized water signal *versus* the inverse local transmitter reference. (A) Reference signal from the external phantom S^{ext} for various coil loads (squares) and S_{corr}^{ext} after multiplication with R_{tra}^{ext} (dots). S_{corr}^{ext} monitors the impedance of the loaded coil [eq. (5)]. A change of 5% in S_{corr}^{ext} remained over the *in vivo* TG range. (B) Reference signal from the external phantom S^{ext} for the 17 subjects. The calibration experiment is indicated by the open diamond. The fitted proportionality constant is indicated by the dotted line. Signals in A and B are not to scale due to hardware changes. (C) Tissue water content [TWC, eq. (10)] estimated external referencing without local sensitivity correction. The lines indicate the fitted proportionality constants (ins GM: filled squares and bold line; pmp GM: open squares, dashed line; pa WM: open diamonds and dotted line)

Table 1. Tissue water in three different brain regions as estimated from the T_2 measurement of the localized water signal^a and sources of signal variations^b obtained from the water signal

	Insular GM	Parietal GM	Parietal WM
<i>Tissue water content</i> ^c (%)			
(1) External reference and local R_{tra} ($n = 11$): ^d	73.8 ± 2.6	73.3 ± 1.9	62.9 ± 0.9
(2) Without external reference: ^e	70.7 ± 2.7*** ^g	69.4 ± 1.4***	60.3 ± 0.9***
(3) Without local R_{tra} : ^f	69.7 ± 3.8*	76.1 ± 2.3***	65.5 ± 2.1**
Repetitive study ($n = 5$)	71.9 ± 1.8	75.0 ± 1.3	63.3 ± 0.7
T_2 of tissue water (ms)	78.3 ± 3.1	77.3 ± 2.6	79.1 ± 1.6
CSF signal/partial volume s_{CSF}	5.0–13.2% (8%)	7.2–16.5% (9%)	1.3–5.6% (4%)
R_{tra}^{ext}/R_{tra}	0.868–1.031 (20%)	0.982–1.062 (8%)	0.986–1.076 (9%)
R_{tra}^{extg}	2.57–3.22 (23%)	2.40–3.07 (23%)	2.40–3.22 (30%)

^a Values are given as mean ± SD.

^b Range of values (and corresponding range of signal variation).

^c Values [eq. (10)] are corrected for T_2 relaxation, CSF contribution and flip angle deviation.

^d Quantification based on eq. (6) combining external reference and the local reference.

^e Obtained by omitting the external reference signal $S^{ext} \cdot R_{tra}^{ext}/V^{ext}$ in eq. (6).

^f Obtained by omitting the R_{tra}^{ext} and R_{tra} in eq. (6).

^g Significance levels of a paired two-sided t -test against the combined Method 1 are indicated by asterisks: * $p < 0.05$; ** $p < 0.01$; *** $p < 0.001$.

the coil center. Multiplication resulted in a difference of 2.5% between the corrected signals. Closer to the coil center the positive deviation decreased with the RF gradient.

A wide range of coil loads was realized by increasing the distance of a high load phantom from the coil center. The resonance frequency of the water signal varied by less than 50 Hz. The external reference signal S^{ext} was linear to $1/R_{tra}^{ext}$ over a wide range of coil loads ($r = 0.998$ as indicated in Fig. 5A), but showed a considerable increase for small loads. S_{corr}^{ext} changed by 5% over the TG range observed for human subjects.

Variations of the local RF field *in vivo*

The external reference measurement showed the variation of B_1 with head size at a reproducible position in the coil. TG was found to be between 76 and 102 in adult subjects, which corresponded to R_{tra}^{ext} between 2.40 and 3.23, i.e. a range of 30% (Fig. 5B). The corresponding variation in S^{ext} was well correlated ($r = 0.97$) and reduced the coefficient of variation (CV) of S_{corr}^{ext} from 8.8% to 2.3%. The range of the TG series was chosen to satisfy sufficient overlap with the signal maximum for RF loads observed on human subjects. Higher TG values were avoided, because for α approaching 180° the signal showed nonlinear deviations from the $\sin^3\alpha$ dependence due to stronger excitation at the margins of the VOI. Systematic deviations from the $\sin^3\alpha$ curve over the range of the TG series were found to be smaller than the experimental error *in vivo* (Fig. 4C). R_{tra} could be reproduced within 1.5% on the same VOI *in vivo*, even if single outliers were present.

R_{tra}^{ext}/R_{tra} is a measure for the sensitivity difference between the VOI and a reference position in the coil (defined by the external phantom). Figure 5C shows the

concomitant change of the TWC (Table 1, method 3 as defined below) in the three regions. These were larger in the insular region (16% interval) than in the parietal regions (8% interval in GM, 9% in WM). Except for pmp GM, R_{tra}^{ext}/R_{tra} varied over a wider range than CSF partial volume and thus proved, to be the second biggest source of signal variation (Table 1). On average, R_{tra}^{ext}/R_{tra} was 9% lower in insular GM than in parietal GM ($p < 0.001$, unpaired two-sided t -test).

Tissue water content and metabolite concentrations

For comparison with previously published work and demonstration of systematic effects (as in Danielsen *et al.*⁸) we applied different correction methods to the data. Method 1 is our combined correction as given in eq. (6). Method 2 corrects by the principle of reciprocity, but is based on the local B_1 alone [omitting the external reference in eq. (6)]. Method 3 is the common external reference method, without accounting for local B_1 [omitting R_{tra} and R_{tra}^{ext} in eq. (6)]. The flip angle correction and the correction for CSF partial volume were retained. For a synopsis of the results for the three regions with sources of signal variation see Table 1. Without the external reference (Method 2) the average TWC is shifted to significantly lower values for all three regions alike ($p < 0.001$, unpaired two-sided t -test). The standard deviations (SD) did not increase. Ignoring local B_1 (Method 3) resulted in regionally dependent changes. SDs increased for all three regions, most prominently in parietal WM. The reproducibility study was performed after replacement of the RF preamplifier, which caused a nominal decrease of 'institutional' signal units by 35%. External referencing yielded results that were consistent with the study group (Tables 1 and 2). Local sensitivity

Table 2. Concentrations of main metabolites (tNAA, tCr, Cho) in three different brain regions as determined by LCModel analysis and three different quantification methods

	Insular GM	Parietal GM	Parietal WM
<i>NAA + NAA-glutamate = tNAA</i>			
(1) External reference and local R_{tra} ($n = 11$)	10.32 ± 0.37	10.40 ± 0.61	10.15 ± 0.46
(2) Without external reference	9.86 ± 0.39***	9.87 ± 0.72***	9.74 ± 0.44***
(3) Without local R_{tra}	9.97 ± 0.66	10.82 ± 0.71 ***	10.50 ± 0.46*
Repetitive study ($n = 5$)	9.68 ± 0.53	10.52 ± 0.30	10.87 ± 0.55
<i>Creatine + P-creatine = tCr</i>			
(1) External reference and local R_{tra}	7.02 ± 0.55	6.50 ± 0.74	5.40 ± 0.47
(2) Without external reference	6.96 ± 0.54***	6.16 ± 0.61***	5.08 ± 0.39***
(3) Without local R_{tra}	7.03 ± 0.62	6.75 ± 0.66***	5.48 ± 0.54*
Repetitive study	6.97 ± 0.24	6.85 ± 0.61	5.20 ± 0.47
<i>Choline compounds = Cho</i>			
(1) External reference and local R_{tra}	1.38 ± 0.12	1.15 ± 0.25	1.46 ± 0.15
(2) Without external reference	1.32 ± 0.11***	1.09 ± 0.23***	1.40 ± 0.13***
(3) Without local R_{tra}	1.33 ± 0.14	1.20 ± 0.26***	1.51 ± 0.15**
Repetitive study	1.21 ± 0.07	0.97 ± 0.10	1.30 ± 0.09

^a All values are given in mean ± SD corrected for CSF partial volume and to 90° flip angle. See also legend to Table 1.

correction reduced the SDs of TWC by half, even though the sensitivity differences between the four VOIs were rather small (<3.5%) and did not influence the TWC significantly ($p > 0.05$, paired two-sided t -test).

Table 2 shows the estimated tissue concentrations in millimol/liter (mM) of the main metabolites total N-acetyl-aspartate (tNAA) (including NAA-glutamate), total creatine (tCr) and choline containing compounds (Cho). Significant differences ($p < 0.05$, unpaired two-sided t -test) between the GM regions were found for tCr and Cho, which are higher in the insular region, but not for tNAA. In white matter, creatine was significantly lower than in both GM regions ($p < 0.01$). The somewhat higher Cho concentrations in parietal WM did not reach significance. When applying different correction methods, similar changes of the calculated metabolite concentrations were found as for the tissue water content, but these were still in the range of reported values.²⁻⁷ Although the SD of tNAA concentrations increased markedly in ins GM without local sensitivity correction, tNAA appeared to be of significantly lower concentration than in pmp GM ($p < 0.001$). The differences in tCr and Cho were obscured if the difference in local sensitivity was not accounted for.

DISCUSSION

Tissue water content and metabolites

Previous estimates of TWC in parietal WM and GM, that were measured using the same MR system and localization sequence,¹⁴ could be reproduced within experimental error when the same correction scheme (external reference, method 2) was applied. As the local sensitivity

correction decreased the signal from the parietal regions, somewhat lower estimates were obtained by the combined approach of this study. The white matter VOIs were quite homogeneous, indicated by CVs of 1.5% in the group or 1% in one subject. Thus, it may be possible to detect subtle structural changes in WM on the basis of the TWC. Reversing the argument, the TWC estimate provides an additional control of the quantitation, if there is no major structural variation. The average TWC was the same in both gray matter regions ($p = 0.67$, unpaired two-sided t -test). However, this may not readily be interpreted in terms of structural similarity, because each gray matter VOI contains an individual amount of white matter. The somewhat larger CVs of 3–4% observed in GM (in one subject 1.7% and 2.5% for pmp and ins GM) comprise biological variation, GM/WM proportion and quantification error. The main metabolite concentrations were estimated from single spectra with Cramer–Rao lower bounds between 4% and 16% (as given by the LCModel output parameter % SD). Hence, errors of metabolite concentrations were dominated by the error of spectral analysis, as indicated by the absence of a correlation between tNAA and TWC.

Good agreement between LCModel analysis of 2.0 T and 1.5 T spectra has been shown for parietal WM and GM.¹³ With the slightly T_2 -weighted quantification of metabolites about same tNAA concentrations were found all three regions. Reports of tNAA differences between gray and white matter at short TE ^{5,8,14-16} may be due to signal-to-noise ratio SNR-dependent differences in the baseline estimation or whether partial CSF volume is accounted for. A recent single-volume MRS study of different brain regions¹⁴ revealed higher levels of creatine and cholines in the insular region compared to pmp GM. Calculating average VOI concentrations by

omitting the correction for CSF partial volume [eq. (9)] rendered our data in quantitative agreement with Pouwels and Frahm.¹⁴

Quantification

Least square fit of the flip angle dependence has been found to be the most robust method to calibrate the excitation flip angle in MRI sequences.¹⁷ Since the fit links a number of independent scans, the result is stable to single outliers. However, the $\sin^3\alpha$ dependence of the signal is not strictly valid, because the localized signal is given by integration over the flip angle distribution across the slices. This distribution, however, is known to change nonlinearly with B_1 . Exclusion of high flip angles and the use of RF pulses which have been optimized for 90° flip angle¹⁰ may explain why the $\sin^3\alpha$ dependency is obeyed with acceptable accuracy. A possible systematic shift of the maximum as observed by others (Fig. 2 in Pan *et al.*¹⁵) will cancel by division of R_{tra} and $R_{\text{tra}}^{\text{ext}}$ in eq. (6).

In two aspects the suggested quantification technique is different from methods published so far: first, it corrects for all changes of the sensitivity through a combination of the localized reference method⁷ and the external reference method.^{3–5} Secondly, it relies only on formalized mathematical operations and is, therefore, independent of flip angle calibration or operator adjustments. The flip angle of a modified water suppression pulse has been suggested to correct for local sensitivity.⁷ This flip angle, however, is likely to depend on T_1 and compartmentation of the *in vivo* water signal and gave less precise results (4% CV) for WM water content.

TWC provides the best basis for a comparison of different correction schemes, because of the high SNR and because the biexponential fit provides a correction for T_2 relaxation and CSF partial volume. Metabolite concentrations, however, show inferior reproducibility due to the error introduced by the low SNR of the spectra. The larger CV of metabolite concentrations may have disguised the effects of RF inhomogeneities under *in vivo* conditions.

The comparison between Methods 2 and 3 (Tables 1 and 2) is in accordance with a previous comparison between the external reference and the local reference method for parietal WM and parieto-occipital GM.⁸ As in our study, the local reference method gave smaller variations and the external reference method gave higher concentrations. The higher significance between the local and external reference obtained in this study ($p < 0.002$ of a paired two-sided *t*-test for every metabolite) may be explained by the lack of individual tuning and matching. $S_{\text{cor}}^{\text{ext}}$ of the calibration experiment showed a positive deviation from the proportionality (diamond in Fig. 5B) and rendered $S_{\text{cor}}^{\text{ext}}$ (and thus Z) at the upper end of the range obtained in subject examinations. Thus, the *in vivo* experiments were systematically underestimated if $S_{\text{cor}}^{\text{ext}}$

was ignored. The relative SDs did not improve, probably because irreproducible susceptibility effects from the water/glass/air interface give rise to additional errors.

The regional sensitivity difference between VOI and external phantom ($R_{\text{tra}}^{\text{ext}}/R_{\text{tra}}$) depends on the positioning of the head relative to the coil's RF field, and may thus vary with subject and the coil used. The largest range of B_1 differences from the external phantom was observed in insular GM. This region is located somewhat more lateral and inferior than the parietal regions and is more susceptible to off-center inhomogeneity of the RF coil. These may impose larger variation and reduce the sensitivity. Local sensitivity correction proved not only crucial for comparison with the external reference, but also the comparison between different regions, here exemplified by insular and parietal cortex. Ignoring B_1 inhomogeneity resulted in anti-intuitive findings like reduced tNAA and TWC in the insular region. On the other hand, significant differences in Cho and tCr were obscured. Local sensitivity correction proved to be beneficial for both the precision and the accuracy of the quantification at 1.5 T and for a commercial head coil. It may be especially useful for higher field strengths and rf coils of inferior homogeneity.

CONCLUSION

Fitting the signal dependence around the 90° maximum of the localized STEAM signal was found to be a robust, time efficient and user-independent way to determine a linear reference (R_{tra}) for the local sensitivity of the MRS signal. Precision and accuracy of the estimated metabolite concentrations can be improved by applying a correction for local sensitivity, especially in lateral and inferior regions. This should be combined with an external reference measurement to avoid systematic shifts of the estimated concentrations. If the loaded coil network is not individually tuned and matched, this is particularly important for the calibration on model solutions, where coil load and impedance may differ from human subjects. Although the observed regional B_1 differences are hardware dependent, their effect should be carefully considered before regional concentration differences may be interpreted in terms of underlying physiological or pathological conditions.

REFERENCES

1. Hoult DI, Richards RE. The signal-to-noise-ratio of the nuclear magnetic resonance experiment. *J. Magn. Reson.* 1976; **24**: 71–85.
2. Hoult DI, Deslauriers R. Elimination of signal strength dependence upon coil-loading—an aid to metabolite quantitation when the sample volume changes. *Magn. Reson. Med.* 1990; **16**: 418–424.
3. Hennig J, Pfister H, Ernst T, Ott D. Direct absolute quantification of metabolites in the human brain with *in vivo* localized proton spectroscopy. *NMR Biomed.* 1992; **5**: 193–199.
4. Ernst T, Kreis R, Ross BD. Absolute quantification of water and

- metabolites in the human brain. I. Compartments and water. *J. Magn. Reson. B* 1993; **102**: 1–8.
5. Kreis R, Ernst T, Ross BD. Absolute quantification of water and metabolites in the human brain. II. Metabolite concentrations. *J. Magn. Reson. B* 1993; **102**: 9–19.
 6. Michaelis T, Merboldt K-D, Bruhn H, Hänicke W, Frahm J. Absolute concentrations of metabolites in the adult human brain *in vivo*: quantification of localized proton MR spectra. *Radiology* 1993; **187**: 219–227.
 7. Danielsen ER, Henriksen O. Absolute quantitative proton NMR spectroscopy based on the amplitude of the local water suppression pulse. Quantification of brain water and metabolites. *NMR Biomed.* 1994; **7**: 311–318.
 8. Danielsen ER, Michaelis T, Ross BD. Three methods of calibration in quantitative proton MR spectroscopy. *J. Magn. Reson. B* 1995; **106**: 287–291.
 9. Frahm J, Merboldt K-D, Hänicke W. Localized proton spectroscopy using stimulated echoes. *J. Magn. Reson.* 1987; **72**: 502–505.
 10. Webb PG, Sailasuta N, Kohler SJ, Raidy T, Moats RA, Hurd RE. Automated single-voxel proton MRS: technical development and multisite verification. *Magn. Reson. Med.* 1994; **31**: 365–373.
 11. Klose U. *In vivo* proton spectroscopy in the presence of eddy currents. *Magn. Reson. Med.* 1990; **14**: 26–30.
 12. Provencher SW. Estimation of metabolite concentrations from localized *in vivo* proton NMR spectra. *Magn. Reson. Med.* 1993; **30**: 672–679.
 13. Helms G. Analysis of 1.5 Tesla proton MR spectra of human brain using LCMoDel and an imported basis set. *Magn. Reson. Imag.* 1999; **17**: 1211–1218.
 14. Pouwels PJW, Frahm J. Regional metabolite concentrations in human brain as determined by quantitative localized proton MRS. *Magn. Reson. Med.* 1998; **39**: 53–60.
 15. Pan JW, Twieg DB, Hetherington HP. Quantitative spectroscopic imaging of the human brain. *Magn. Reson. Med.* 1998; **40**: 363–369.
 16. Doyle TJ, Bedell BJ, Narayana PA. Relative concentrations of proton MR visible neurochemicals in gray and white matter in human brain. *Magn. Reson. Med.* 1995; **33**: 755–759.
 17. Foxall DL, Hoppel BE, Harihanan H. Calibration of the radio frequency field for magnetic resonance imaging. *Magn. Reson. Med.* 1996; **35**: 229–236.